NUMERICAL AND EXPERIMENTAL STUDY OF BUCKLING OF ADVANCED FIBRE COMPOSITE CYLINDERS UNDER AXIAL COMPRESSION

R S PRIYADARSINI[1], V KALYANARAMAN[2]
Department of Civil Engineering, Indian Institute of Technology, Madras
Chennai 600 036, India
[1]priyadarsini_rs@yahoo.com; [2]kalyan@iitm.ac.in

and

S M SRINIVASAN[3]
Department of Applied Mechanics, Indian Institute of Technology, Madras
Chennai 600 036, India
[3]mssiva@iitm.ac.in

ABSTRACT

Advanced lightweight laminated composite shells are increasingly being used in modern aerospace structures, for enhancing their structural efficiency and performance. Such thin-walled structures are susceptible to buckling when subjected to static and dynamic compressive stresses. In this paper, details of a numerical (FEM) and an experimental study on buckling of carbon fibre reinforced plastics (CFRP) layered composite cylinders under displacement and load controlled static and dynamic axial compression are reported. The effects of different types of loadings, geometric properties, lamina lay-up and amplitudes of imperfection on the strength of the cylinders under compression are studied. Accurate measurement of imperfections in the cylindrical surface is carried out in the specimens tested. It is shown that the buckling behaviour of thin composite cylindrical shells can be evaluated accurately by modeling measured imperfections and material properties in FEM.

1. Introduction

Composite cylindrical shells, used in weight sensitive structures such as aircraft fuselages, submarine hulls and space launch vehicles, are essentially subjected to membrane stresses and are efficient due to the high strength to weight ratio and stiffness to weight ratio.[1] However, they are vulnerable to instabilities (buckling) when subjected to static or dynamic compressive stresses.[2] The introduction of faster supersonic aircrafts, ballistic missiles and launch and re-entry vehicles has necessitated investigations of dynamic buckling. The growing demand for safety of transport vehicles has also had a strong impact on the increasing interest in dynamic buckling.[3]

A cylindrical shell under compression in the meridional direction can fail by overall buckling (global/Euler), local buckling or the material strength being reached. Various failure mechanisms of composite cylindrical shells, as affected by initial geometric imperfections, boundary conditions, lamina stacking sequence, anisotropic coupling effects and load eccentricity, were identified by Weaver,[2] in terms of laminate configurations and shell proportions. The buckling response of the shells is very sensitive to changes in boundary conditions. A significant discrepancy between theory and experiment is possible in the case of cylindrical shells unless the boundary and loading conditions are accurately modeled and the initial geometric imperfections are precisely taken into consideration in any theoretical model. Unlike shells made of

isotropic materials, composite cylindrical shells could experience failure due to a stronger coupling between membranes and bending strains. Degradation of the buckling strength of composite laminates may also occur due to delamination resulting from poor fabrication.[3]

While numerous experimental and theoretical studies are available on the buckling and post-buckling characteristics of isotropic shells including the effects of geometric imperfections, relatively few have reported studies on the buckling behaviour of laminated composite shells. Many of the experimental studies were only on curved composite laminate panels so as to avoid the high cost and complexities involved in fabrication and testing of the full composite cylindrical shells.[3]

Tennyson[4] reviewed, in detail, the theoretical and experimental investigations on buckling of laminated cylinders. This included the effects of material and geometric non-linearities and boundary conditions on buckling strength of the shell, as well as correlation studies between theory and experiments. Similar investigations on filament wound glass-epoxy thick and thin cylinders (having various radius to thickness ratios) with circumferential and helical windings were described in.[5-7] Axial compression tests on these shells revealed that for some winding angles compressive load induces shear resulting in new buckling failure modes. Shells having smaller radius to thickness ratios experienced catastrophic material failure under shear stress while the large ones exhibited failure by the classical diamond shaped shell buckling mode. The experimental buckling loads were about 65-85% of the theoretical linear elastic buckling loads.

Papers dealing with the effect of imperfection in laminated composite structures[8] are available in literature, based on Koiter's[9] imperfection shell theory. These indicate reasonably good estimates of the buckling loads for axial compression and bending loading. The main difficulty in developing post buckling theories, required to assess the imperfection sensitivity of composite cylindrical shells, is the lack of reliable imperfection data.[3] In the absence of such data, approximate knock down factors are used to find the critical buckling load.

In the seventies and eighties, several analytical and experimental studies were conducted on the buckling behaviour of composite cylinders fabricated from prepregs, considering the effect of assumed axi-symmetric initial geometric imperfections having the same RMS values amplitudes as measured.[10-11] The discrepancy between theory and experiments were about 20%. Studies, [12-13] also revealed that sensitivity to geometric and loading imperfections was influenced by the laminate lay-up and that a strong interaction exists between shape imperfections and loading imperfections.

A numerical study [14] on the effect of thickness variation on the stability of composite cylindrical shells under axial compression showed that thickness variation over the cylinder can greatly reduce the classical buckling load especially when the wave number of the thickness variation is twice that of the classical buckling mode. A new approach to determine the lower bound of the load carrying capability for thin-walled composite shells is presented,[15] which has the potential to provide an improved and less conservative shell design in order to reduce weight and cost of thin-walled shell structures made from composite material.

The stacking sequence of the plies influences the coupling (off diagonal) terms of the stiffness matrix of the laminate and consequently the buckling strength of the laminate. Symmetric laminates do not exhibit bending-membrane coupling, while a balanced lay-up (in which for every θ layer there is a $-\theta$ layer) eliminates extensional-shear coupling. In addition, there is no bending-twisting coupling of stiffness terms for a unidirectional

(only 0°) or cross-ply (0° and 90°) construction. The effect of bending-twisting coupling is not pronounced for a symmetric laminate with a large number of plies. Thus, it is important to differentiate between the different types of laminates to identify the modes of buckling that may be critical.

Weaver *et al*.[16] described experimental investigations on the advantage of using an antisymmetric lay-up for a laminate over a symmetric laminate in spiral buckling modes. They also showed, based on Onoda's solution,[18] that in order to eliminate the anisotropic coupling effects, which lower the buckling loads, a laminate with a minimum of 48 plies is required. But their study ignored the effect of initial imperfections. Wullschleger *et al.* [19] recommended, based on extensive buckling tests and analyses, that for most reliable evaluation of the instability of imperfect CFRP cylinders, proper imperfection measurements, with a nodal resolution in the order of the mesh size used for the non-linear prebuckling analyses, are needed. Bisagni[20] reported the correlation within 15 to 20% between the numerical and experiments in composite shell buckling, using the measured imperfections in the finite element model.

Most research on instability of shells in the past two decades was confined to static loading conditions only. Instability under dynamic conditions has become important with the introduction of faster supersonic aircrafts, ballistic missiles and launch and re-entry vehicles. The term 'dynamic buckling' has in particular been used in literature to indicate two essentially different phenomena. One is associated with the response of structures to the action of oscillating loads, where the transverse vibration becomes unacceptably large at critical combinations of load amplitude, load frequency and structural characteristics. For a structure with an axial force, buckling can occur at sufficiently small values of axial force when the loading frequency equals twice the natural bending frequency of the structure. Because of the similarity to vibration resonance this behaviour is known as *vibration buckling.* The second dynamic buckling phenomenon relates to the behaviour of structures subjected to impact loads. It represents the loss of stability or the deformation of a structure to unbounded amplitudes as the result of a transient response to an applied impact load, i.e. *dynamic buckling under impact loads.* [3]

Limited research has been carried out in literature on the dynamic stability of cylindrical shells in which membrane action is considered to be the unperturbed state of stress.[21-25] Most of them have considered simply supported end conditions while both ends fixed condition would be an assumption closer to reality in practice. Nagai and Yamaki [26] found that the classical membrane approaches are inaccurate when the vibration contribution of the axisymmetric modes is not negligible. As in the case of static instability, geometric imperfections reduce the ultimate load. [27-32]

The studies on the instabilities of thin advanced fibre composite cylindrical shells made by hand lay-up of prepregs under static and dynamic conditions are very limited. Even these indicate discrepancy between the analytical prediction and the experimentally observed behaviour. This paper presents details of a numerical (FEM) and experimental study on CFRP composite cylinders under displacement and load controlled static and dynamic axial loading conditions. It is shown that the buckling behaviour of thin composite cylindrical shells can be predicted by accurate measurement of initial geometric imperfections, modeling it appropriately in FEM and by using measured material properties. The experimental study is on carbon fibre composite cylinders made from eight layers of unidirectional carbon-epoxy prepregs with a symmetric balanced lay-up of $[0°/45°/-45°/0°]_s$ made using hand lay-up of prepregs.

Details of a FEM based parametric study on the effects of specimen geometry and lay-up sequences are included. The effect of loading duration on the dynamic buckling load of the shell structure is also studied and reported. Method of manufacture, imperfection measurement and results of the tests on a few CFRP cylinders under static and dynamic axial compression are presented. They are compared with FEM results generated using ABAQUS. It is shown that the buckling characteristics of thin composite cylindrical shells can be predicted with less than 5% error.

2. Parametric Study using FEM

Before arriving at the dimensions and the lay-up sequence of the experimental specimen, some parametric studies are required to be carried out to determine the effect of length (L) to mean radius (r) ratio (L/r), mean radius to thickness (t) ratio (r/t) and the lay-up sequence on the buckling strength of cylindrical shell. A readily available mandrel used for the fabrication of the specimen, fixed the specimen inner diameter to be 300mm. The specimens were made up of pre-impregnated carbon-epoxy tapes of width 300mm and thickness 0.125mm. The buckling and post-buckling behavior of the CFRP cylindrical shells were studied numerically using ABAQUS (Version 6.8), a general purpose finite element program with linear static, dynamic and non-linear analysis capabilities[33]. The complete shell geometry was modeled, as required in composite laminates exhibiting coupling,[16] using 4-noded S4R shell elements, with reduced integration. These shell elements having six degrees of freedom at each node, are free from shear locking and hour glass mode. [33] In the model, all the six degrees of freedom (three rotations and three translations) were arrested at one (supported) end of the shell and at the other end (loaded) all the degrees of freedom, except the axial deformation degree of freedom, were arrested. The results of the parametric studies are given below.

The properties of the prepreg as supplied by the manufacturer were used in the model (Table 1).

Table 1. Mechanical properties of the CFRP

Longitudinal Tensile modulus, E_l (MPa)	Transverse Tensile modulus, E_t (MPa)	In-plane shear modulus, G_{12} (MPa)	Poisson's ratio, ν_{12}	Density (Kg/m^3)	Thickness (mm)
134780	9250	4800	0.286	1700	0.125

2.1 *The effect of L/r and r/t ratios on the linear elastic buckling load*

The different values of L/r ratio (ranging from 0.5 to 3.0) and r/t ratio (ranging from 60 to 300) were chosen, keeping the inner diameter of the shell constant at 300mm and varying the length and the thickness of the shell. Four layer balanced lay-up sequence (0°/45°/-45°/0°) and a symmetric balanced lay-up (45°/-45°/-45°/45°) were chosen for the study. The variation of the linear elastic buckling stress (P_{cr}/A) with respect to L/r and r/t ratio is shown in Fig.1 for both the lay-up sequences. It is seen that the influence of L/r, for shells having $L/r \geq 1$ on the buckling stress is hardly noticeable in each of the lay-up sequence. Whereas, in both lay ups the effect of radius to thickness (r/t) is quite evident. This implies that the buckling strength of the shell depends mainly on the radius to thickness ratio and the lay up sequence of lamina in the composite laminated shell in the range of

parameters studied here. Hence, the choice of the length in the study can be freely made for $L/r \geq 1$ and the thickness may be chosen based on the behaviour and strength requirements to be studied.

2.2 *Influence of lay-up sequence on the elastic buckling load and buckling mode*

A parametric study was carried out to determine the buckling mode shapes corresponding to different lay-up sequences and also the lay-up corresponding to the maximum linear elastic buckling load of a cylindrical shell, of inner diameter of 300 mm, 400 mm length and 1mm thickness (made of 8 unidirectional prepregs). The lay-up sequences chosen for the study and the corresponding buckling mode shapes and the linear elastic buckling loads obtained are shown in Fig.2. The fibre orientations are measured from the meridional direction of the shell and the stacking sequence is ordered from the innermost to the outermost layers.

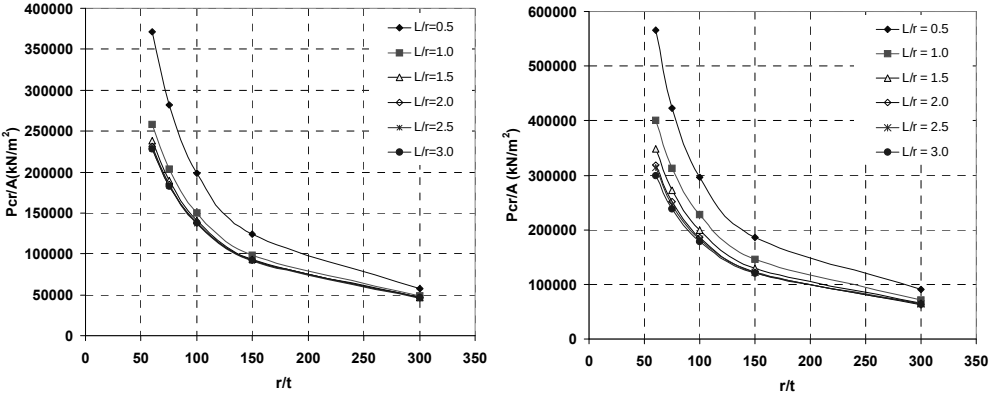

(a) (45°/-45°/-45°/45°)

(b) (0°/45°/-45°/0°)

Fig.1 Variation of P_{cr}/A for various L/r and r/t ratios for two different lay-up sequences

It is seen that even if the overall dimensions, the length and the thickness remain the same, the variation in the lay-up sequence of the prepregs can lead to considerable variation in the elastic buckling load and the buckling mode. Most of the specimens experience spiral mode of buckling, excepting the specimen having anti-symmetric lay-up, which experiences axisymmetric buckling mode and the specimen having orthogonal lay-up, which experiences the diamond shaped buckling mode. The shell having lay-up (0°/0°/30°/-30°/-30°/30°/0°/0°) with fibres oriented closer to the meridional direction does not have the largest elastic buckling strength. It is also seen that as the anisotropy factor increases the pitch of the spiral buckling mode decreases.

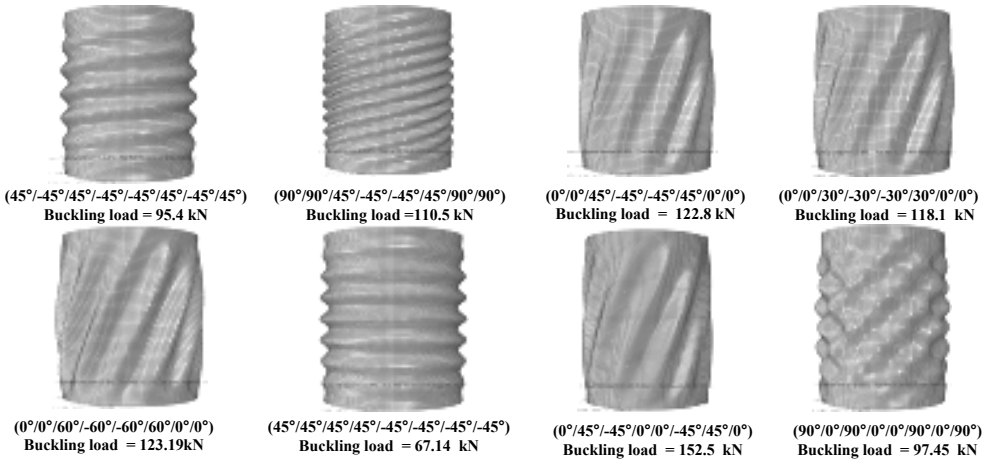

Fig. 2 Mode shapes and buckling loads for different lay up sequences

3. Experimental Study

Based on the parametric study, a carbon composite cylindrical shell specimen with 300 mm inner diameter, 400 mm length, 1mm thickness and a lay-up sequence of $[0°/45°/-45°/0°]_s$ has been chosen for the experimental study. The choice is based on the maximum value of the elastic buckling strength, elimination of bending-extensional coupling and extension-shear coupling and the minimum bending-twisting coupling. The composite laminate for the cylindrical shell is designed so that material failure does not occur before the buckling failure, by fixing the buckling strength of the shell well below the compressive strength of the laminate. Four specimens were fabricated from pre-impregnated unidirectional carbon-epoxy (T300/914UD) tapes of width 300mm and thickness 0.125 mm. Thus the nominal thickness of all the cylindrical shells was 1 mm, resulting in the nominal radius-to- thickness ratio of 150.5.

3.1. *Specimen Preparation*

An available mandrel of 450mm length and 300mm outer diameter and a taper of 1mm in the diameter over its length was used to make the cylindrical shell specimens of 400mm height and 300mm inner diameter.

The composite cylindrical shell specimens were manufactured by hand lay-up procedure on the mandrel. Before wrapping the layers of prepreg around the cylindrical mandrel, the mandrel surfaces were thoroughly cleaned with acetone to remove any dust, dirt or rust. Then, one layer of Teflon coated release film was placed over the mould surface of the mandrel and the reference line for 0^0 in the axial direction of the mandrel was marked on the surface.

The individual layers were then placed to give the final laminate and this was accomplished by wrapping each layer individually around the mandrel tightly by hand and pressing with rollers, while staggering the joints of each layer evenly around the

circumference. The entire surface after lay-up was first covered by one layer of release film followed by two layers of bleeder (Air weave, N4). Then it was covered by two layers of breather (Air weave N7 or A-3000-7) material. Then a vacuum bag was mounted with sealant putty and fixed with three nipples (two for suction vents and one for pressure measurement) and a thermocouple for monitoring the product temperature while curing. The setup was checked for a vacuum of 0.8bar (min) and the product were given consolidation under vacuum for minimum duration of 30 minutes. After this the product was placed in an autoclave for curing under combined pressure and vacuum. The following cure cycle was followed.

a) Switch on the vacuum pump and maintain a minimum vacuum of 0.8 bar inside the vacuum bag for 10 minutes.
b) Apply a pressure of 4 bar on the surface of the bag while maintaining the vacuum of 0.8 bar inside the bag.
c) Switch on the heater and increase the temperature at 3^0C / min, to achieve the maximum temperature of 177 ± 3^0 C.
d) Hold the product at 177 ^{0}C for duration of 2 hours under the combined pressure and vacuum.
e) Then gradually decrease the temperature to 60^0C in one hour.
f) Switch off the heater and vacuum pump after the product reaches 60^0 C.

The advantage of following combined pressure and vacuum curing is that the strength properties of the laminate can be enhanced. After curing, the shells were ultrasonically inspected to ensure that no voids or delaminations were present in the specimen. The two ends of the shells were cut flat, parallel and normal to the axis of the cylinder using diamond cutting tool, prior to testing, so as to ensure uniform contact on the specimens.

3.2. *Material Characterization*

A flat plate laminate having the same lay-up sequence, made using the same material and process as well as cured under the same conditions as that of the cylindrical specimens was used to find out the actual material properties of the laminate in the shell as fabricated. Strips cut as per the ASTM D6272-02 standards from the laminate along the fibre direction (0°) and perpendicular to the fibre direction (90^0), were subjected to four point bending test. Three strips were tested to obtain properties in the orthogonal directions. From these tests the flexural rigidity of the laminated plate was obtained, using which the longitudinal and transverse moduli of a single ply were calculated as given in Table 2. The other properties were taken as specified by the manufacturer. The values of the moduli as obtained from tests were higher as compared to the standard values provided by the manufacturer. This may be because the values provided by the manufacturer were based on the tensile test on vacuum cured unidirectional laminate whereas the laminate tested in the study was cured under combined vacuum and pressure. These test values were used in the subsequent finite element model of the specimen.

Table 2. Tested Mechanical properties of the CFRP laminate

Longitudinal Tensile modulus, E_ℓ (MPa)	Transverse Tensile modulus, E_t (MPa)	In-plane shear modulus, G_{12} (MPa)	Poisson's ratio, ν_{12}	Density (Kg/m^3)	Thickness (mm)
148500	9850	4800	0.286	1700	0.125

3.3. *Preparation of the Specimens for the Buckling Test*

The cylinders were to be tested for uniform compression in the meridional direction with their ends clamped, allowing only the axial deformation to take place. The clamped end constraint was achieved by bonding the ends of the shell specimen to the end steel plates using Araldite, an epoxy resin. The machined steel end plates had a diameter of 360 mm and a thickness of 25mm. In order to get proper seating of the specimen, a circular groove of depth 5mm and width 5mm was cut on one surface of each steel plate in which the specimen ends were seated. This would also avoid the possibility of "brooming" of fibres due to the end loading. In order to ensure uniformity in loading, care has taken to make the loading surface of the end plate and the inner surface of the groove to be parallel (see Fig.3a).

A total of 22 numbers of 10mm strain gauges were bonded to the inner and outer surfaces of the cylindrical specimen to obtain both membrane and bending strain in the shell. Out of these, 20 were linear strain gauges and two were strain rosettes. The pairs of gauges (on the inner and outer surfaces) were oriented 90° apart in the meridional and circumferential directions at the middle of the cylinder as shown in Fig 3b. The meridional strain gauges were used to measure the axial strains and flexural strains along the meridion, to get an indication of the buckling of the shell. The circumferential gauges were employed to measure hoop and bending strains in that direction. In addition, six more strain gauges, three each at the top and bottom ends of the cylindrical specimens, were provided on the outer surface in the meridional direction, distributed at 120° around the circumference. These were used to check the uniformity in the applied loading/ deformation.

3.4. *Measurement of Imperfections*

Before the strain gauges were mounted, the outer surface initial imperfections were measured except the first specimen (trial run). For this purpose the specimen was mounted on a turn table, which can be rotated about the axis of the shell. Externally a 20 mm range linear variable differential transducer (LVDT), having a least count of 1/1000 mm, was mounted on a support so as to contact the outer surface of the shell in the radial direction and be able to move up and down parallel to the meridional axis. The LVDT was connected to a data acquisition system and the data was recorded at points on the outer surface of the shell at 5° apart in the circumferential direction and 10 mm in the meridional direction. Using the data on radial variation of the surface, the mean cylinder diameter was determined to obtain least square of the error. The measured coordinates of the specimen surface's points were further modeled in MATLAB to reconstruct the real shape of the imperfections in the specimen. This is plotted for the specimen 2 in Fig. 4. The shell surface is opened out on to a horizontal plane. The imperfection in the cylinder is taken as the radial distance between the best-fit cylinder and the actual shell surface as measured.

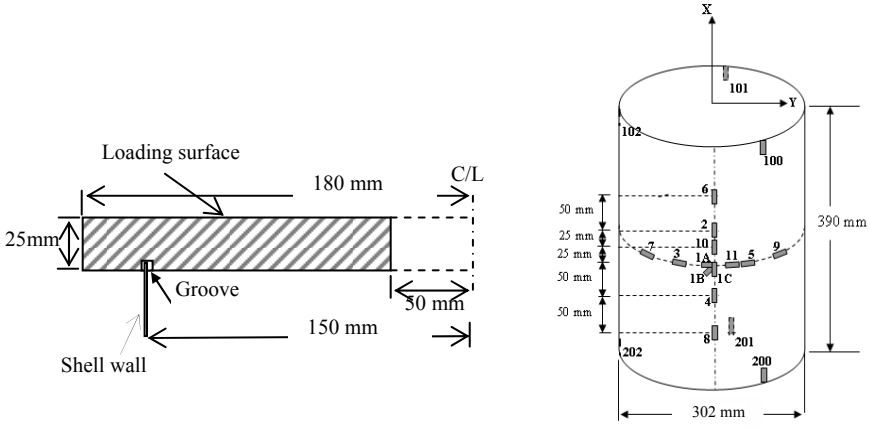

(a) Details of steel cover plate (b) Strain gauge locations

Fig.3. (a) The details of the covering plates attached to the top and bottom of the shell. (b) The locations of strain gauges on the inner and outer faces of the shell

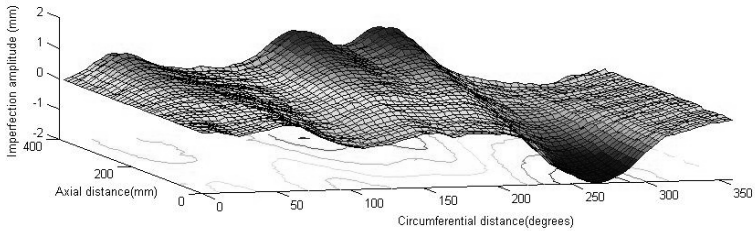

Fig. 4 Variation of initial imperfection of the outer surface of the cylindrical shell specimen 2

3.5 *Test Procedures*

One each of load controlled and displacement controlled static buckling tests and two dynamic buckling tests under displacement control were carried out on the laminated composite cylindrical shell specimens, as described below.

3.5.1 *Load controlled static buckling test*

The initial geometric imperfection of this specimen was not measured before the test. The set up for the load controlled static buckling test is shown in Fig. 5. The CFRP cylindrical shell was subjected to static axial compression under load control by a hydraulically operated compression testing machine of 600 T capacity. The specimen was placed between the two heads of the compression testing machine, which has a moving bottom head and a fixed top head. In order to accurately ascertain the axial load applied on the specimen, a

Fig.5. Final set up for the load controlled static buckling test

load cell was placed between the specimen and the top head.

For measuring the axial deformation of the shell and also to verify the concentric and uniform loading, three LVDT's, equally spaced around the circumference, were used to measure the relative deformation between the two end plates. Initially to ensure proper contact and uniformity of pressure around the circumference, a load of around 1.5 tonnes was applied and reduced to a small initial value. The load was increased thereafter at a slow rate in steps until failure. The readings of the load cell, LVDTs and the strain gauges were recorded by means of a data acquisition system, MGC plus, after every load increment of around 5 kN.

When the load reached 77.1 kN, the shell buckled suddenly with a loud noise into the classical diamond mode with large diamond-shaped buckles uniformly distributed around the cylinder surface. The buckled mode shape of the cylindrical shell specimen after the ultimate load is shown in Fig. 6. On inspection of the cylinders after their buckling revealed no brooming or crushing at their ends.

Fig.6 Buckling modes obtained in the load controlled test

But on slight increase of the load, crushing of the fibres occurred along the meridional direction at the central height. The specimen failed due to shell buckling followed by crushing of the ply in the 0° direction in the unstable post-buckling range due to the combined effect of membrane compression and bending in the meridional direction.

3.5.2 *Displacement controlled static buckling test*

The specimen for the displacement controlled static test was prepared using the same procedure as explained in the load controlled test. The controlled displacement in the axial direction was applied using a 50T servo controlled actuator (MTS), which is capable of applying both static and dynamic loadings. The test set up is shown in Fig. 7. The actuator was mounted vertically on a 200T testing frame vertically by means of bolts. The actuator had an inbuilt load cell which was also corroborated using a 25T load cell loaded parallely. The specimen was placed on a steel pedestal placed below the actuator and attached to a strong floor using pre-tensioned bolts. The servo controlled actuator, the specimen and the bottom reaction table were aligned perfectly so as to ensure true axial loading on the specimen, which was ascertained during test using LVDT and strain gauges in the meridional direction.

The actuator was controlled through a digital controller which was also connected to a PC. Using the controller desired displacement was applied to the actuator in steps and the command as well as the response data was recorded on a personal computer. The axial deformation of the shell was increased at the rate of 0.01mm per minute, initially. Corresponding change in readings of the strain gauges, load cell and the LVDT's were also acquired by the data acquisition system.

Fig. 7 Buckling mode under displacement controlled static buckling test

Till the load reached 98 kN, the shell showed no sign of buckling. But when it reached 98.6 kN, it suddenly buckled with a loud noise into a diamond pattern mode shape. Two half waves along the axial direction and six full waves along the circumferential direction, uniformly distributed over the entire circumference of the shell was observed. At the point of buckling a sudden drop of load was observed from 98.6 kN to 36 kN. The displacement was further increased at the same rate to study the post-buckling behaviour of the composite cylindrical shell. The load could be increased only up to 42 kN. After that again the load decreased with increase in deformation. A crack was observed in the meridional direction, as in the load control test. Unlike in the load control test, more number of waves uniformly distributed over the entire surface of the shell was observed in the displacement controlled test.

3.5.3 *Displacement controlled buckling test under combined linearly increasing and harmonic loading*

The specimen manufacture and test set up was the same as that of the displacement controlled static buckling test. The axial deformation was increased in the form of

$$\Delta(t) = \Delta_1(t) + \Delta_2(t) \text{ Sin } \omega t \qquad (1)$$

where $\Delta_1(t)$ was the linear increment component which was increased from 0 to 2 mm over a predefined time duration as discussed below and $\Delta_2(t)$ Sin ωt was the harmonic part with the applied displacement at a frequency of 50 Hz. The loading frequency was chosen as 50 Hz since it is the dominant frequency in a recorded rocket thrust data. The amplitude of the harmonic component $\Delta_2(t)$ was taken as 10% of the static component at that instance of time. According to vibration buckling, structures subjected to periodic axial loads may undergo dynamic buckling at a lesser load than its static buckling load if the loading frequency was close to twice the natural bending frequency of the structure. However, in our case the axial loads are of higher amplitude and the loading frequency is less than the natural bending frequency of the structure which is 482 Hz (obtained from a frequency extraction analysis). Two such experiments were conducted with the 2mm displacements being achieved in 2s and 5s durations.

In both the cases, the initial imperfection study was conducted. The maximum amplitude of imperfection from the mean cylinder was 1.7576 mm. The desired displacement by the actuator was applied through the digital controller. It was observed that in both the cases the shell buckling behaviour was similar to that under the static test. The ultimate load was 99.8 kN and the shell buckled with a loud noise into classic diamond wave pattern with 6 full waves around the circumference in the case of 2s load duration. Whereas in the case of 5s load duration, the ultimate load observed was 98.2 kN and the shell buckled into diamond pattern with 6 full waves around the circumference and two half waves along the meridional direction. Fibre breakage occurred in the meridional direction in the post-buckling region of buckling for 5s duration whereas no fibre breakage occurred in the 2s duration test. After unloading, both the shells returned back to their original shape indicating that the observed behaviour was essentially elastic, except in the damaged region. The buckling patterns obtained from the experiments are shown later in section 5. The details of the load versus strain curves for all the above mentioned experiments are also given in section 5 along with the numerical results.

4. Finite Element Analysis

Finite element analyses of the composite cylindrical shell specimens were carried out to study their buckling characteristics under uniform axial compression and calibrate the FEM model results with experimentally observed results. Three types of analyses, namely linear static (Eigen value) buckling analysis, non-linear static (Riks method) analysis and non-linear dynamic analysis were carried out using ABAQUS.

In the experiments, the specimens were attached to end plates in a circular groove of 5 mm depth, at the two ends. Therefore the actual specimen length of 390 mm between plates, inner diameter of 300 mm and thickness of 1mm were considered in the finite element model. The nodes at one end of the shell were considered as fully fixed against translation and rotation and all the degrees of freedom except the displacement in the meridional direction of the nodes at the other loaded end of the shell were restrained to model the loading through the circular end plate. The tapering of 1mm in the diameter over the length of the cylindrical shell specimen was also modeled and the results were compared with that of the model without tapering. It was found that the tapering makes no difference in the buckling load as obtained from the linear buckling analysis. So for all further analyses, the finite element model without the small taper was considered. Two types of loading conditions were considered corresponding to the static loading case, namely load controlled and displacement controlled. For the dynamic analyses, only displacement controlled type of loading was considered. In both the cases, the axial compression was applied as a uniformly distributed load/displacement around the circumference in the meridional direction. The material properties of the laminate obtained from material characterization tests were used for the analyses.

The complete shell geometry was modeled, as required in composite laminates exhibiting coupling. [16] The cylindrical specimens were modeled using 4-noded S4R shell elements, with reduced integration. In the model all the six degrees of freedom (three rotations and three translations) were arrested at one (supported) end of the shell and at the other end (loaded) all the degrees of freedom except the axial deformation were arrested.

4.1. *Linear Elastic Instability (Eigen Value) Analysis*

Linear elastic buckling loads of composite cylindrical shells can be evaluated by Eigen value analysis. Generally this analysis is carried out on the perfect model without considering imperfections. However in this study the linear elastic instability analysis has been carried out both on models without and with imperfections, to study its effect on the linear elastic buckling load. The buckling load predicted by this method on model without imperfections normally gives an idea of the upper limit of the ultimate strength of the cylindrical shell and is usually much higher than that from tests and non-linear FEA because of imperfection effects. In a shell with imperfections, the actual ultimate load and the buckling mode may be considerably different from that obtained by the linear buckling analysis of model without imperfections. But the linear instability load serves as a guideline for carrying out the non-linear analysis and is computationally much simpler and faster than the non-linear analysis.

The Eigen value analysis has been carried out using the finite element code ABAQUS/Standard. Before carrying out the analysis, a mesh refinement study was performed to ensure that satisfactory convergence has been achieved in the finally used model. From the study, a mesh with 13320 elements, 180 along the circumferential direction and 74 along the meridional direction, was chosen as it was a good compromise between accuracy and CPU time. This model and the previous model with 170 elements along the circumferential direction and 69 elements along the meridional direction had a convergence error of 0.4%. The buckling load of shell obtained from the linear elastic analysis was 165.77 kN both for load controlled and displacement controlled analyses.

4.2. *Non-linear Static Analysis*

In linear elastic bodies, the displacements are proportional to the applied loads. But in the case of buckling, even if the stress-strain relation remains linear, large deformations and the changing geometric configuration cause the structure to behave non-linearly. The actual behaviour can be predicted accurately only by the non-linear analysis, even though it is more time consuming and computationally more expensive.[20]

In ABAQUS/Standard, the non-linear analysis was carried out using the modified Riks procedure, to solve the non-linear governing equations.[33-34] In this method, a single equilibrium path is defined in terms of the nodal variables and the loading parameter (load/displacement). The basic algorithm follows the Newton method. Finer increments are used as the load/displacement approaches the ultimate value and the basic approach in non-linear buckling analysis is to increment the applied load/displacement until the solution does not converge.

The buckling loads and the mode shapes obtained from the linear elastic static buckling analysis and the geometric non-linear static analysis without any initial geometric imperfections are shown in Fig. 8. The two buckling modes are different even though the difference between the elastic buckling load and ultimate loads is marginal.
Subsequently imperfection in the form of first linear buckling mode was assumed with different amplitudes varying from *0.0 t* to *1.0 t*, where *t* is the shell thickness, to study their effect on the ultimate strength. Figure 9a shows the knockdown factors (the ratio of the ultimate strength of cylinders (P_u) with imperfections to the linear elastic buckling strength of the perfect cylinder, (P_{cr}) corresponding to different imperfection amplitudes. The ultimate load is taken as the maximum limit loads in case of specimens with unstable

post-buckling (load shedding) behaviour ($\delta_0/t \leq 0.5$). When such a behaviour was not observed, the ultimate load is taken as the load at which the curve deviates from almost a linear path. The non-dimensionalized axial load with respect to P_{cr} versus the non-dimensionalized axial displacement, Δ/L, graphs obtained from the geometric non-linear analysis are shown in Fig. 9b. It indicates the imperfection sensitivity of the cylinder caused by the unstable post-buckling behaviour of the cylinders subjected to axial compression. As expected the buckling loads of the composite cylindrical shells decreases as the amplitude of the imperfection increases and this rate of decrease is more for changes in imperfection amplitudes at lower values.

(a) Linear buckling analysis, P_{cr} = 165.77 kN (b) Non-linear static analysis, Pu = 164.3 kN

Fig.8. Buckling modes and loads obtained through static analysis of models without imperfections.

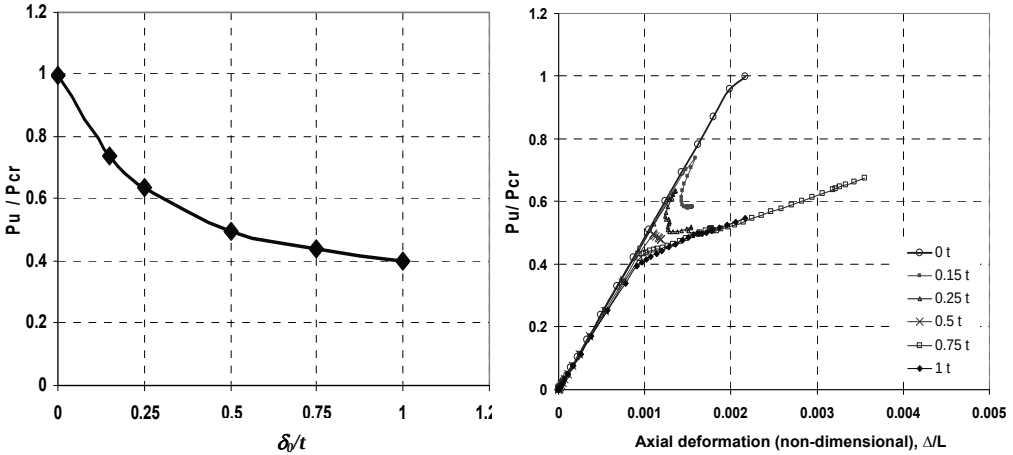

(a) Ultimate strength

(b) Variation of axial load with axial deformation (non-dimensional) for various imperfection amplitudes (δ_0)

Fig. 9 Effects of imperfections (δ_0)

For the purpose of the comparison of the FEM results with the experimental values, non-linear analyses were also carried out corresponding to the measured imperfections, by superposing them on the cylinder to create the actual geometry with imperfections for the analysis. A cylindrical coordinate system was employed and the radial distance of the nodal coordinate was taken as $R = r_0 + \delta$, where r_0 is the mean radius of the best fit cylinder and δ is the imperfection amplitude.

4.3. *Dynamic Analysis*

ABAQUS/Explicit was used for carrying out the dynamic analysis, where the equations of motion governing the dynamics of the cylinders were solved by an explicit integration operator. Here the integration time step was automatically calculated by the code. The load/displacement was imposed as per the actual rate of loading in the test. In these analyses imperfections corresponding to the measured values from the imperfection test results were used. The applied displacement was linearly varied over a given time duration in the case of ramp loading (slow-compression). A cyclic component of displacement with magnitude equal to 10% of the instantaneous ramp load and frequency equal to 50 Hz was superposed in case of combined linearly increasing and harmonic displacement (Eqn.1).

The axial deformation, $\Delta(t)$, was applied for different durations in the range of 0.001-10 seconds in order to study the effect of load duration on the ultimate strength of the shell. The results corresponding to the specimen 4 are tabulated in Table 3 as an example for the loading as specified by Eqn. 1. It may be noted that the limit loads of a cylinder subjected to periodic loading decreases quickly with increasing load duration and converge to the static buckling load. If the time duration is lesser or near to the natural period of the shell, the dynamic buckling strength of the shell is higher than the static buckling strength. Otherwise it converges towards the static buckling strength.

5. *Comparison of Experiments with Analyses*

Comparisons of the results for the three analysis methods, (namely, the linear elastic instability analysis, the non-linear static analysis and non-linear dynamic analysis) with the corresponding experimental data of all the four specimens tested are presented in Table 4. The following observations can be made for the first two specimens subjected to static axial compression based on the comparison.

- For the first specimen linear elastic instability analysis predicts a buckling load of 165.77 kN and a spiral buckling mode with waves covering the entire circumference of the shell with n=11, where n is the number of full sine waves. Experimentally, the observed ultimate load was found to be 77.1 kN. This reduction could be attributed to the presence of initial geometric imperfections, not accounted for in the linear elastic analysis and non-linear static analysis (see Fig. 8 and Table 4). The non-linear analysis of the first specimen predicts a buckling mode (axi-symmetric) different from the linear elastic analysis (see Fig.8), but the ultimate load is closer (within 0.5%) to the linear elastic buckling load. The buckling mode observed in test was diamond shape with five full waves running uniformly around the circumference of the shell. From Fig.11 it can be inferred that the actual amplitude of the initial imperfection, not measured in specimen 1, may have been around 0.5 t.

Table 3 Effect of load duration on the Ultimate load of the shell (Specimen 4)

Duration of loading (s)	P_u/P_{cr}	Axial displacement at buckling , Δ/L
0.001	1.33	0.00310
0.0025	1.11	0.00236
0.005	0.96	0.00203
0.01	0.86	0.00178
0.1	0.71	0.00135
1	0.66	0.00128
2	0.65	0.00128
3	0.64	0.00123
5	0.63	0.00123
10	0.60	0.00118

Table 4. Comparison of the loads from the FE analysis and experiments.

	Specimen1 (*perfect*) (Load controlled)	Specimen 2 (*imperfect*) (Displacement controlled)	Specimen 3 (*imperfect*) $\Delta(t)$, 2 sec duration	Specimen 4 (*imperfect)* $\Delta(t)$, 5 sec duration
Linear elastic instability analysis (P_{cr})	165.77 kN	115.5kN	-	-
Non-linear static analysis (P_u)	164.3 kN	108 kN	-	-
Non-linear dynamic analysis (P_u)	-	99 kN	105.8 kN	103.3 kN
Experiment (P_u)	77.1 kN	98.6 kN	99.8 kN	98.2 kN

- Since the initial geometric imperfections were modeled in case of specimen 2, even the elastic critical load predicted by the linear elastic analysis has reduced (compared to the value of the Specimen 1).
- The non-linear static analysis incorporating measured initial imperfection in the model could predict the ultimate load of the second specimen very near to the experimental value with less than 10% error. Even though the buckling mode obtained from both the analysis and experiment (Fig. 10(a) and Fig. 7) was of diamond shaped, unlike in the non-linear analysis model, more number of waves was running uniformly around the circumference of the shell in experiment. This shows that even after introducing the actual imperfections in the model and using the actual material properties of the laminate, the non-linear static buckling analysis fails to predict the actual buckling mode of the composite cylindrical shells as seen in experiment, although the strength predicted is reasonably accurate.

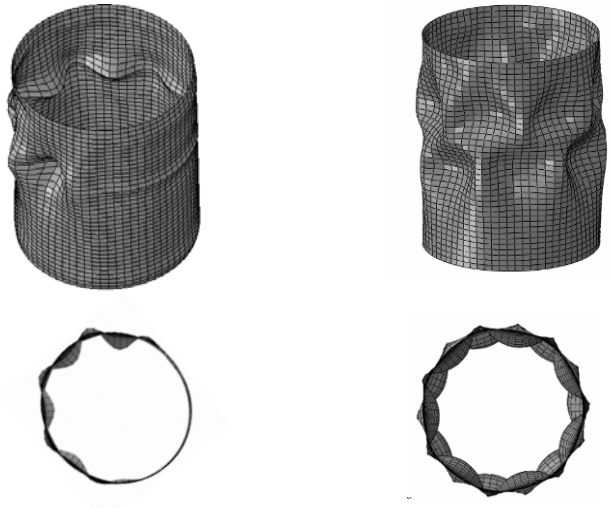

(a) Displacement controlled non-linear static analysis

(b) Dynamic analysis

Fig.10. Buckling Modes of the Specimen 2 under displacement control

- The dynamic analysis of a slow compression test of the second specimen predicts the actual buckling behaviour of the shell in terms of the load and buckling mode (Fig. 10(b) and Fig. 7 and Table 4) very closely as observed in the experiment. It predicts an ultimate load of 99 kN and the buckling mode as diamond pattern with two tiers of wave running uniformly around the circumference of the shell as observed in experiment.

The non-dimensionalized plots of axial load vs. axial deformation obtained from the non-linear static analysis, dynamic analysis and the experiment for specimen 2 are compared in Fig. 12. From the figure it is seen that, even an initially imperfect shell behaviour is almost linear and the shell retains its original shape till it buckles. After reaching the ultimate load, a sudden drop in the load occurs with a large axial shortening. At this point the shell snaps into a *diamond pattern or a checker board pattern*. It can also be noted that in the prebuckling stage and up to the ultimate load comparison of the experiment and analyses results are in good agreement. However, in the post buckling range, the comparison is not as good, because of the unstable post buckling behaviour of shells. The dynamic analysis using ABAQUS/Explicit gives more accurate results compared to non-linear static instability analysis using ABAQUS/Standard in the static buckling case. This study thus gives an insight that the method of analysis also plays a major role in the prediction of the buckling behaviour of the shell subjected to axial compression.

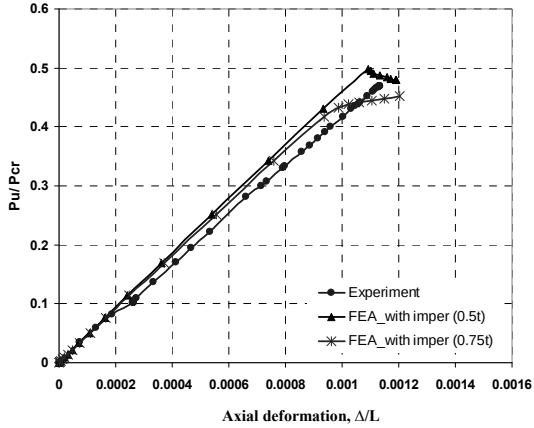

Fig. 11. Comparison of the Load Vs Axial deformation (non-dimensional) plots obtained from FEA for the specimen 1 for different imperfection amplitudes with the experiment.

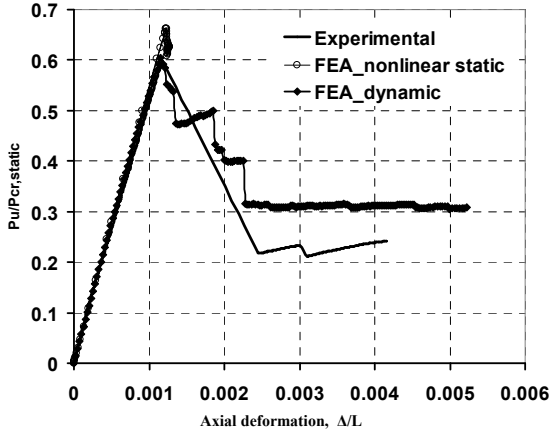

Fig. 12 Comparison of axial load vs. axial deformation (non-dimensional) for Specimen 2

Fig. 13 shows the comparison between the variation of axial strains and hoop strains with the axial load at the mid height of the shell from the non-linear static and dynamic analyses and experimental results. The non-linear analyses are able to predict the behaviour of the shell in the experiment very accurately. Even though the buckling modes obtained from the non-linear static and dynamic analyses are different, the strains are more or less the same. This may be because of the lack of any bending until the critical load reaches and the sudden unstable post buckling behaviour.

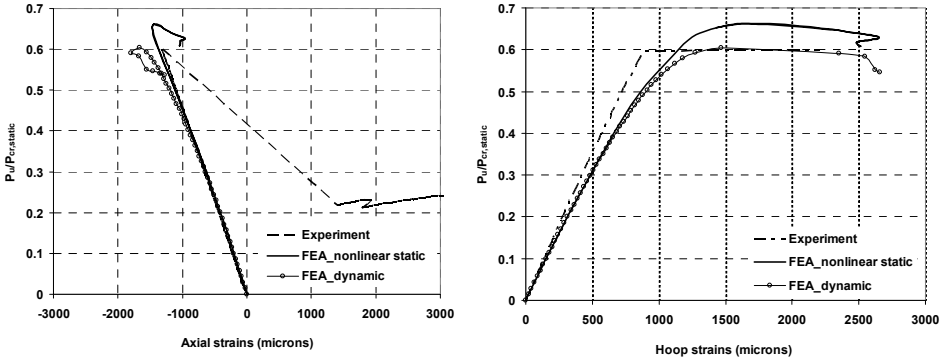

Fig. 13 Comparison of the axial and hoop strains with axial load (Specimen 2)

The following observations are made from the comparison of the analyses and experiments of the specimens (3 & 4) subjected to combined linearly increasing and harmonic axial compression.

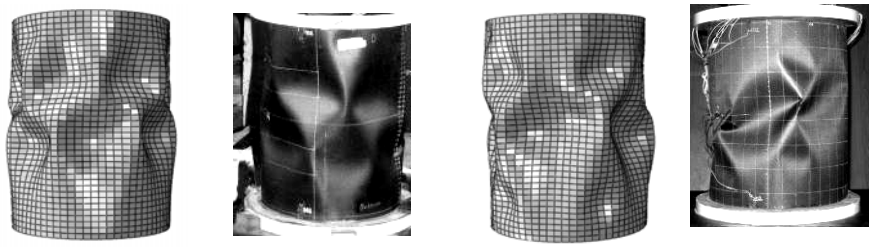

(a) Load duration = 2 sec (b) Load duration = 5 sec

Fig.14 Buckling modes obtained under dynamic loading for different time durations

- The dynamic analyses of the specimens 3 and 4 with the actual measured imperfections predict the ultimate strength and the buckling mode very close to the experimentally observed behaviour with an error of around 5% (see Table 4 and Fig. 14).
- Comparison of the non-dimensionalized axial load vs. axial displacement plots of the specimen 4 (see Fig. 15, as a sample) from the analysis and experiment shows a good agreement in the prebuckling region and up to the ultimate load. But, there exists a difference in the post buckling region due to the unstable post buckling behaviour of shells.
- Analyses done to determine the effect of load duration on the ultimate strength of the thin cylinder shows that (see Table 3), the ultimate strength decreases quickly with increasing load duration and approaches to the static ultimate load for long duration periodic loads. If the load duration is lesser than or near the natural period of the shell, then the ultimate load capacity of the shell under periodic loading is higher than the static ultimate strength.

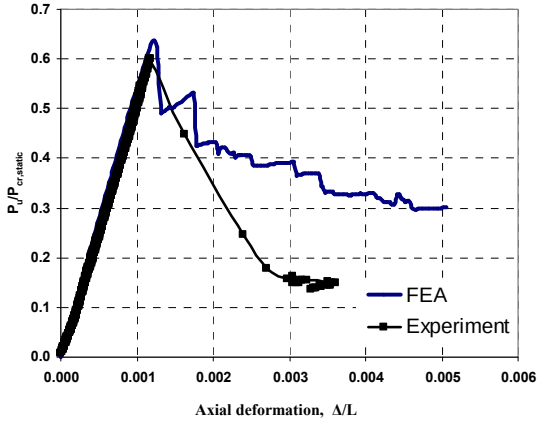

Fig. 15. Comparison of Axial load Vs Axial displacement for Specimen 4

In this study it is shown that, using the tested properties of the laminate of the shell along with the actual imperfections, we can model the buckling behaviour of the shell more accurately (with an accuracy of 95-100%) than has been reported in the literature until now.

6. Summary and Conclusions

The paper deals with the numerical (FEM) and experimental study on the buckling and post-buckling behaviour of thin CFRP cylindrical shells under static and dynamic axial compression under load controlled and displacement controlled conditions of loading. Three different types of finite element analyses: linear static instability analysis (Eigen value), non-linear static instability analysis (Riks method) using ABAQUS/Standard and a dynamic analysis using ABAQUS/Explicit were carried out to model the actual experiments.

It is shown that the ultimate strength is affected by the method of loading (static, harmonic), the lay up sequence, radius to thickness ratio, and geometric imperfections. The effect of the ratio of the length to the radius is negligible.

It is seen that although the mode shapes obtained from linear elastic analysis, non-linear analysis under static and dynamic loading conditions can be very different, the ultimate strength is not greatly influenced by these, as long as the loading frequency (under harmonic loading) is sufficiently far from the natural frequency of the shell. Dynamic analysis of a slow compression test using ABAQUS/Explicit proved to be more effective in predicting the ultimate load as well as the buckling mode and the post-buckling behavior of the shell.

The results from this study indicate that numerical modeling can be used to evaluate the buckling strength accurately, provided the material properties and initial imperfections are properly modeled.

List of symbols used

P_{cr}	=	linear elastic buckling load
P_u	=	ultimate strength at failure
A	=	area of cross section of the cylinder
Δ	=	axial deformation of the cylinder
δ_0	=	amplitude of initial imperfections (corresponding to first buckling mode)
L	=	total free length of cylinder between supports

References

[1] R. M. Jones, *Mechanics of Composite Materials* (McGraw Hill, 1975).

[2] P.M. Weaver, Design of laminated composite shells under axial compression. *Composites Part B* **31**(8) (2000) 669-79.

[3] J. Singer, J. Arbocz, and T .Weller, *Buckling Experiments, Experimental Methods In Buckling Of Thin-Walled Structures, Volume 2, Shells, Built-Up Structures, Composites And Additional Topics*, (John-Wiley, Hoboken, NJ, USA, 2002)

[4] R.C. Tennyson, Buckling of laminated composite cylinders: A review, *Composites* (1975) 17-24.

[5] M.F. Card, The sensitivity of buckling of axially compressed fibre-reinforced cylindrical shells to small geometric imperfections, *NASA TMX-61914* (1969)

[6] J. Tsai, A. Feldman, and D.A. Stang, The buckling strength of filament wound cylinders under axial compression, *NASA, CR-266* (1965).

[7] H.T. Hahn, D. W. Jensen, S.J. Claus and P.A. Hipp, Structural design criteria for filament wound composite shells, *NASA CR-195125* (1994).

[8] A.W. Leissa, Buckling of laminated composite plates and shell panels, *Report AFWAL-TR-85-3069* (AF Wright Aeronautical Laboratories, 1985).

[9] W.T Koiter, On the stability of elastic equilibrium. *Delft: Doctoral Thesis*, 1945. English Translation: AFFDL-TR-70 25, (1970).

[10] R.C. Tennyson, K.H. Chan, and D.B. Muggeridge, The effect of axisymmetric shape imperfections on the buckling of laminated anisotropic circular cylinders, *Transactions of the Canadian Aeronautics and Space Institute* **4**(2) (1971).

[11] R.C. Tennyson, and J.S. Hansen, Optimum Design for Buckling of laminated Cylinders, in Collapse*: The Buckling of Structures in Theory and Practice* (J.M.T. Thompson and G.W. Hunt eds., Cambridge University Press, Cambridge, 1983), pp. 409-429.

[12] B. Geier, H. R. Meyer-Piening, and R. Zimmermann, On the influence of laminate stacking on buckling of composite cylindrical shells subjected to axial compression, *Composite Structures* **55** (2002) pp.467-474.

[13] B. Geier, H. Klein and R. Zimmermann, Buckling tests with axially compressed unstiffened cylindrical shells made from CFRP, in: Buckling of Shell Structures, on Land, in the Sea and in the Air, *Proceedings of the International Conference,* J.F. Jullien, ed., INSA Lyon , Elsevier Applied Science, London, New York (September 1991), pp. 498-507.

[14] Y. W. Li, I. Elishakoff and J. H. Starnes Jr, Axial buckling of composite cylindrical shells with periodic thickness variation**,** *Computers and Structures*,**56**(1) (1995) 65-74.

[15] C. Hu¨hnea, R. Rolfesa, E. Breitbachb and J. TeXmerb, Robust design of composite cylindrical shells under axial compression — Simulation and validation, *Thin-walled structures* **46** (2008) 947-962.
[16] P.M. Weaver, J.R. Driesen and P. Roberts, Anisotropic effects in the compression buckling of laminated composite cylindrical shells, *Composites Science and Technology* **62** (2002) 91-105 .
[17] P.M. Weaver, J.R. Driesen, and P. Roberts, The effects of flexural/twist anisotropy on compression buckling of quasi-isotropic laminated cylindrical shells, *Composite Structures* **55**(2) (2002) 195-204.
[18] J. Onoda, Optimal laminate configuration of cylindrical shells for axial buckling, *AIAA Journal* **23**(7) (1985) 1093.
[19] L. Wullschleger and H. R. Meyer-Piening, Buckling of geometrically imperfect cylindrical shells- definition of a buckling load, *International Journal of Non-linear Mechanics* (37) (2002) 645-657.
[20] C. Bisagni, Numerical analysis and experimental correlation of composite shell buckling and post-buckling, *Composite: Part B* **31** (2000) 655-667.
[21] V.V Bolotin, *The dynamic stability of elastic systems* (Holden-day, San Francisco, 1964).
[22] J. C. YAO, Dynamic stability of cylindrical shells under static and periodic axial and radial loads. *AIAA Journal* **1** (1963), 1391-1396.
[23] J. D. Wood and L. R. KOVAL, Buckling of cylindrical shells under dynamic loads AIAA *Journal* **1** (1963) 2576-2582.
[24] A. Vijayaraghavan and R. M. Evan-Iwanowski, Parametric instability of circular cylindrical shells, *Journal of Applied Mechanics, Transactions of the American Society of Mechanical Engineers* **E.34** (1967) 985-990.
[25] L. R. KOVAL, Effect of longitudinal resonance on the parametric stability of an axially excited cylindrical shell, *Journal of the Acoustical Society of America* **55** (1974) 91-97.
[26] K .Nagai and N. Yamaki, Dynamic stability of circular cylindrical shells under periodic compressive forces, *J. Sound and Vibration* **58**(3) (1978) 425–41.
[27] R.S Roth and J. M. Klosner, Non-linear response of cylindrical shells subjected to dynamic axial loads. *AIAA J* **2** (1964) 1788–94.
[28] Y. S. Tamura and C. D. Babcok, Dynamic stability of cylindrical shells under step loading, *J. Appl Mech* **42** (1975) 190–4.
[29] N.Yamaki, *Elastic stability of circular cylindrical shells* (Amsterdam: North-Holland; 1984).
[30] F. Pellicano and M. Amabili, Stability and vibration of empty and fluid-filled circular cylindrical shells under static and periodic axial loads, *Int. J Solids and Structures* **40** (2003) 3229–51.
[31] M. Amabili and M. P. Pai¨doussis, Review of studies on geometrically non-linear vibrations and dynamics of circular cylindrical shells and panels, with and without fluid structure interaction, *Appl Mech Rev* **56** (2003) 349–81.
[32] G. Catellani, F. Pellicano, D. Dall'Asta, and M. Amabili, Parametric instability of a circular cylindrical shell with geometric imperfections, *Computers and Structures* **82** (2004) 2635-2645.
[33] ABAQUS Manuals, Version 6.8 (Hibbitt: Karlson and Sorensen, Inc.)

[34] Riks, E., An incremental approach to the solution of snapping and buckling problems, *Int. J Solids and Structures* **15** (1979)529-51.